JEE Journal of Ecological Engineering

Journal of Ecological Engineering 2023, 24(1), 336–348
https://doi.org/10.12911/22998993/156150
ISSN 2299–8993, License CC-BY 4.0

Received: 2022.10.12
Accepted: 2022.11.18
Published: 2022.12.01

Carboxymethyl Cellulose Nanoadsorbent for Remediation of Polluted Water

Khairiah Khairiah[1,2], Erna Frida[1*], Kerista Sebayang[1], Perdinan Sinuhaji[1], Syahrul Humaidi[1], Ridwanto[2], Ahmad Fudholi[3], Putut Marwoto[4]

[1] Department of Physics, FMIPA, Universitas Sumatera Utara, Jl. Bioteknologi I Kampus USU Medan 20155, Indonesia

[2] Universitas Muslim Nusantara Al Washliyah, Jl. Garu II A No. 93, Medan Amplas, Kota Medan, Indonesia

[3] Solar Energy Research Institute, Universiti Kebangsaan Malaysia, 43600, Bangi, Selangor, Malaysia

[4] Physics Department, Faculty of Mathematics and Natural Science Universitas Negeri Semarang, Sekaran-Gunungpati 50229, Semarang, Indonesia

* Corresponding author's email: ernafridatarigan@usu.ac.id

ABSTRACT

The development of nanoadsorbents for remediation of polluted water in order to obtain clean and healthy water quality has been carried out, namely the incorporation of chitosan, magnetic, and activated carbon materials. The activated carbon used is the result of the synthesis of banana peel waste nanocrystals, while the magnetic is Fe_3O_4. The method used in this study is an experimental method with coprecipitation through several stages, namely (1) magnetic synthesis of Fe_3O_4 by thecoprecipitation method, (2) preparation of chitosan solution, (3) synthesis of activated carbon nanocrystals from banana peel waste by the milling process, (4) merger of the three materials, and (5) characterization with SEM/EDX, XRD, FTIR, BET, PSA, TGA, and AAS to test the performance of the material against polluted water. The study found that 210 minutes was the optimal time for the heavy metal ions Fe, Mn, Zn, and Pb to adsorption.The best sample was sample S4 with a ratio of 1:2:2 with adsorption for Zn 92.43%, Fe 95.44%, Mn 89.54%, and Pb 84.38%. For the heavy metal ions: Mn 5624 mg/g, Fe 5849.4 mg/g, Zn 4894.22 mg/g, and Pb 468.2 mg/g, the Langmuir model was used. The adsorption kinetics showed that the reaction order for Pb, Mn, Zn, and Fe ions varied with pseudo-first order and pseudo-second order. Carboxymethyl cellulose nanoadsorbents are effective in remediating the water contaminated with heavy metals, such as Pb, Mn, Zn, and Fe, meeting the environmental health quality standards for water media for sanitation hygiene purposes.

Keywords: banana peel, activated carbon, chitosan, magnetic, nanoadsorbent, remediation of polluted water.

INTRODUCTION

The contamination of the aquatic environment is an interesting environmental issue to be researched. Various efforts have been made to minimize pollution of the aquatic environment, one of which is the adsorption method. Adsorption is an efficient method for removing various heavy metals which is being developed nowadays (Khairiah et al., 2021). Chitosan is one of the often used materials, where the amine (NH_2) and hydroxyl (OH) in high concentrations can bind to metal ions and remove bacteria through coordination mechanisms and electrostatic interactions. However, not all metal ions can be adsorbed on the chitosan material due to poor acid resistance (Olaoye et al., 2020). In addition, it also has a weakness, namely the small adsorption capacity so that other materials are needed to support the performance of this material, namely activated carbon. Activated carbon is a biomass waste that is used as the basic material for making adsorbents, which includes the plants that contain lots of carboxylic acids and hydroxyl groups OH, namely banana peel waste (Alinezhad et al., 2020). On the basis of previous research, activated carbon from banana peel waste has the potential to become an adsorbent material. Activated

carbon as an adsorbent material has a large surface area, quite large pores and is hydrophobic (does not mix with water), can eliminate odors and cloudy colors in polluted water (Safari et al., 2019; Khairiah et al., 2021). Although activated carbon from banana peel waste is a material that is quite potential for adsorption of heavy metal ions, but as an adsorbent material it has several weaknesses, including being difficult to separate in the adsorption process and it cannot be used repeatedly, so modifications are needed with the development of other technologies to assist the separation, namely magnetic technology (Siregar et al., 2021; Yu et al., 2021). The process is carried out with rod magnets so that the adsorbent can be taken and reused repeatedly. The magnetic material used is Fe_3O_4 that is synthesized by the coprecipitation method, which is a bottom-up method of making nanoparticles by involving NH_4OH as the precipitating solution (Hu et al., 2020; Adusei et al., 2022). In this study, the adsorbent was carboxymethyl cellulose (CMC) nanoadsorbent which consisted of 3 types of materials, namely chitosan, magnetic Fe_3O_4, activated carbon from banana peel waste. In turn, the adsorbate (absorbed substance) is a metal ion. The combination of the three materials by using the addition of glutaraldehyde (Gameli et al., 2022; Safari et al., 2019). The addition of glutaraldehyde is a crosslinked agent which is strong enough so that it is expected to increase the adsorption ability of the three materials.

The formation of CMC nanoadsorbent powder is expected to be a new material that can be applied as an adsorbent material in the remediation of polluted water. In the mechanism of the adsorption process, the metal ions dissolved in water bind bi-polar so that they become one unit and become bound or absorbed with CMC nanoadsorbent material; then, for separation with water, assisted separation with a bar magnet at the bottom are employed so that clean water can be obtained (Negroiu et al., 2021; Munagapati et al., 2018). On the surface of the CMC nanoadsorbent with the adsorbate, physical intermolecular forces occur, namely Van der Waals forces and electrostatic interactions. Modifications of chitosan, magnetic CMC, and activated carbon of banana peel waste were used as new adsorbent materials that were cross-linked with hydroxyl (OH) groups that could bind heavy metal ions (Jafer & Hassan, 2019; Tejada-Tovar et al., 2018). The hydroxyl site of the material is a highly reactive group. Thus, it is assumed to be able to form strong intermolecular hydrogen bonds with the induced dipole interaction coordination mechanism.

EXPERIMENTAL PROCEDURE

Syntesis of magnetic Fe_3O_4

At this stage, magnetite (Fe_3O_4) is synthesized using the coprecipitation method. Comparison of FAS (III) and FAS (II) was made 3:1. First, 8.97 g of FAS(III) and 3.18 g of FAS(II) were weighed and then the powder was mixed and added into 150 ml of distilled water until dissolved. Then, it was stirred and added gradually little by little excess 2M NH_4OH solution (pH > 7) and the reaction continued until it reached pH 9 (Annadurai et al., 2018; Khairiah et al., 2021). Then, the solution was heated and stirred using a water bath shaker. The temperature used is 70 °C for 30 minutes. The solution was then allowed to stand and a magnetite precipitate (Fe_3O_4) was formed and then rinsed using distilled water until the pH was neutral according to the pH of the distilled water used. Afterwards, it was dried and then filtered using filter paper and subsequently dried in a desiccator for 24 hours.

Preparation of chitosan solution

A total of 50 mL of 1% acetic acid solution was prepared with a composition of 10 mL of 10% acetic acid added 40 mL of distilled water, then stirred and added 0.5 g of chitosan into 1% acetic acid solution and then stirred until evenly distributed. This mixture is called chitosan solution (Yuvaraja & Venkata, 2016; Abbasi, 2017).

Synthesis of activated carbon nanocrystals from banana peel waste

First, the banana peel was dried with a preparation technique to remove the dirt and impurities attached to the banana peel and reduce the water content. It was then ground with a mortar and pestle, sieve with a sieve, and smoothed again with a blender; then, the banana peel powder was subjected to High Energy Milling (HEM). The milling process was carried out for 24 hours with an interval of 30 minutes for each 90 minute cycle (Chen et al., 2017; Khairiah et al., 2021). Carbonization occurred at low temperature of 250 °C for

10 hours. The results of the carbonization were chemically activated by using a concentrated HCl solution of 25%. The particles and NaOH solution were stirred for 2 hours then the sample was placed into the oven at 80 °C for 4 hours.

Synthesis of incorporation of chitosan, magnetic (Fe_3O_4), activated carbon

The 0.5 g chitosan solution that had been made was then stirred using a magnetic stirrer and 2 mL of 50% glutaraldehyde was added, stirred for 30 minutes and then stirred again manually when 0.5 g of magnetite and carbon were added until well mixed and soaked in 1M NaOH solution for 12 hours, then washed using distilled water until neutral and afterwards stored in a desiccator to dry and a chitosan-magnetite-carbon adsorbent was formed. Furthermore, the characterization of SEM/EDX, XRD, FTIR, PSA, BET/BJH, TGA and AAS was carried out to test the adsorption performance (Gameli et al., 2022; Petcharoen & Sirivat, 2012). Comparison of the variations of the three materials to be synthesized with seven samples can be seen in Table 1. The seven samples comprised: S1 included 0.5 g of chitosan, 0.5 g of magnetic and 0.5 g of banana peel carbon. S2 is 0.5 g of chitosan, 0.5 g of magnetic and 1.0 g of banana peel activated carbon. S3 is 0.5 g of chitosan, 1.0 g of magnetic and 1.0 g of banana peel activated carbon. S4 is 0.5 g of chitosan, 1.0 g of magnetic and 1.0 g of banana peel activated carbon. S5 is 1.0 g of chitosan, 1.0 g of magnetic and 0.5 g of banana peel activated carbon. S6 is 0.5 g chitosan, 1.0 g magnetic and 0.5 g banana peel activated carbon and the last S7 is 1.0 g chitosan, 0.5 g magnetic and 1.0 g banana peel activated carbon.

Table 1. CMC sample comparison

Sample	Comparison		
	Chitosan	Magnetic (Fe_3O_4)	Activated carbon
S1	1	1	1
S2	1	1	2
S3	2	1	1
S4	1	2	2
S5	2	2	1
S6	1	2	1
S7	2	1	2

Characterization

Furthermore, characterization was carried out using SEM/EDX, XRD, FTIR, PSA, BET/BJH and AAS to test water quality. SEM/EDX characterization was used to investigate the morphology and identify the clearer composition of banana peel activated carbon, Fe_3O_4 nanoparticles and CMC material nanoadsorbent. XRD characterization was used to investigate the phase formed from Fe_3O_4 magnetic powder and CMC material nanoadsorbent powder. FTIR characterization was used to investigate the functional groups formed on Fe_3O_4 magnetic and CMC material nanoadsorbent powder. PSA characterization was used to investigate the particle size of Fe_3O_4 magnetic powder and CMC material nanoadsorbent powder. BET/BJH characterization was used to investigate the pore size and surface area of banana peel activated carbon and CMC nanoadsorbent material. TGA characterization was used to investigate the change in weight % with temperature.

Adsorption performance test with AAS

AAS characterization was used to investigate metal compounds contained in untreated water and treated using the CMC material nanoadsorbent. Quality tests that have been performed using the CMC material nanoadsorbent to investigate the efficiency value of the CMC material nanoadsorbent towards the recovery/remediation of polluted water were calculated and analyzed (Yu et al., 2021; Feng et al., 2021).

Determination of Adsorption Contact Time and Adsorption Model for heavy metals Fe, Mn, Zn and Pb – the removal of heavy metals was initially carried out using the batch method. The adsorption of heavy metals Fe, Mn, Zn and Pb (1,351; 1,210; 17,403 and 0.17 mg/L) by adsorbents was carried out simultaneously in 50 mL polluted water at neutral pH 7 and at room temperature (27 °C). The observed adsorption contact times were 30, 60, 90, 120, 150 and 180 min with a stirring speed of 150 rpm. From the process of determining the optimum contact time, it is also possible to analyze the adsorption mechanism. Determination of heavy metal content was made using AAS. Determination of the adsorption isothermic model was performed using the Langmuir and BET models (Annadurai et al., 2018; Nithya & Sudha, 2016).

Effect of pH on the adsorption of heavy metals Fe, Mn, Zn and Pb – the adsorbent was placed into a glass beaker then 50 mL of water contaminated with heavy metals Fe, Mn, Zn and Pb was added (initial concentrations of each metal in polluted water: 1,351; 1,210; 17,403 and 0.17 mg/L). The pH of the polluted water was regulated by adding HCl (0.1 M) and NaOH (0.1 M). pH variation of 3, 4, 5, 6, 7 and 8. The time used was the optimum contact time in procedure a, the adsorption temperature was kept at room temperature with 150 rpm stirring (Mahmoudi et al., 2020; Singh et al., 2018).

DISCUSSION

Adsorption process and AAS

In the adsorption process, AAS characterization was used to investigate metal compounds contained in water that had not been treated and had been treated by nanoadsorbent material CMC. Quality tests that have been performed using nanoadsorbent material CMC to investigate the % adsorption of nanoadsorbent material CMC on the recovery/remediation of polluted water were calculated and analyzed with the parameters of contact time, acidity level, stirring speed, adsorption model and adsorption kinetics. The % adsorption for the seven samples with each of the heavy metal ions Fe, Mn, Zn and Pb are shown in Figure 1, 2, 3 and 4.

The concentrations of each heavy metal ion in polluted water were Fe, Mn, Zn and Pb (1,351; 1,210; 17,403 and 0.17 mg/L) and the volume of polluted water was 50 mL, pH 6 and stirring speed of 200 rpm. The figure shows the relationship between contact time and % adsorption of heavy metal ions of Fe, Mn, Zn and Pb that are absorbed, the optimum time is 210 minutes. For Fe ions, the order of samples from the most effective is S4>S3>S1>S5>S7>S6>S2, while for Mn ions it is S4>S3>S1>S5>S6>S7>S2 and for Zn

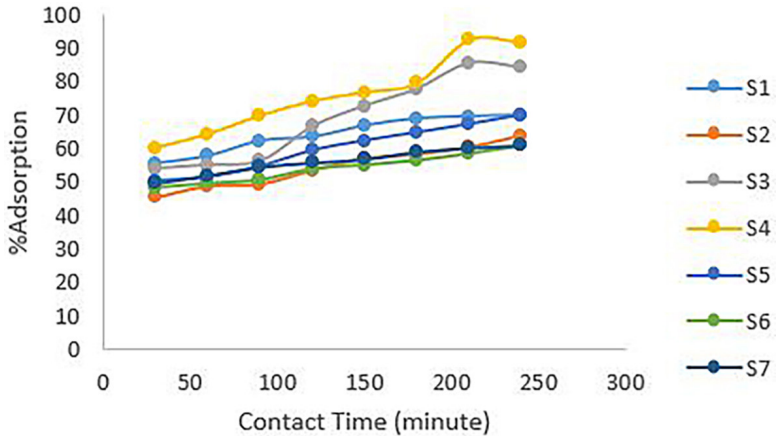

Figure 1. Relationship % adsorption of heavy metal ion Fe in polluted water and contact time

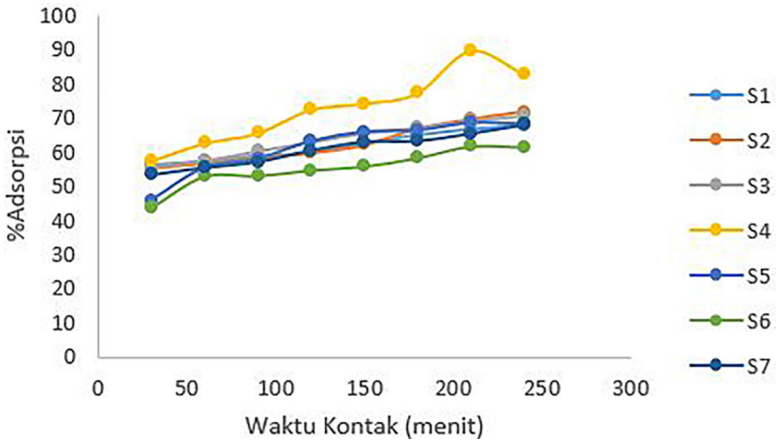

Figure 2. Relationship % adsorption of heavy metal ion Zn in polluted water and contact time

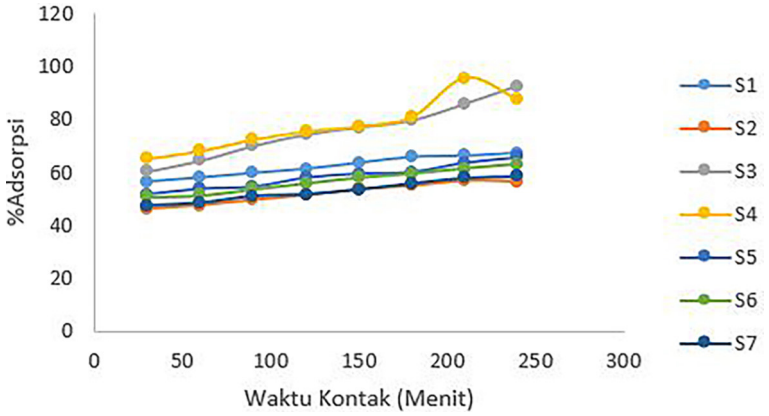

Figure 3. Relationship % adsorption of heavy metal ion Mn in polluted water and contact time

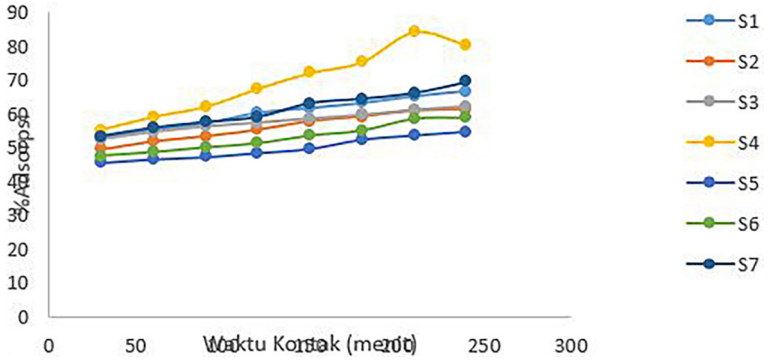

Figure 4. Relationship % adsorption of heavy metal ion Pb in polluted water and contact time

ions it is S4>S3>S1>S5>S2>S7>S6, then for the Pb ions it is S4>S7>S1>S3>S2>S6>S5, so it can be concluded that of the 7 samples of CMC nanoadsorbents, the most effective sample was S4 for each adsorbed heavy metal ion, followed by S3 for Fe, Mn and Zn ions, whereas for Pb ions it was S7. This is because it has the highest % S4 adsorption compared to other samples. Sample S4 is the easiest to experience the phenomenon of diffusion in the heavy metal ion adsorption mechanism of Fe, Mn, Zn and Pb. To ensure the performance of the CMC nanoadsorbent in removing the four heavy metals, it is necessary to compare it with the removal capability by magnetic Fe_3O_4 alone and banana peel activated carbon separately which has been carried out in the previous procedure. Determination of the Langmuir adsorption model of the four heavy metals Fe, Mn, Zn and Pb can be seen in Figure 5 and 6.

The calculation results are shown in the table that the metal ions Fe, Pb, Zn and Mn have a positive increase and tend to follow the Langmuir adsorption model. From Figure 5. and 6 Langmuir adsorption for Fe, Mn, Zn and Pb ions showed a curved graph, this curvature as evidence of surface heterogeneity of the bonding sites of CMC nanoadsorbents. The heterogeneity in the graph models shows the curvature of the isothermal graph as a gentle slope indicating a fairly high and constant adsorption affinity. The maximum adsorption capacity using the Langmuir method is for heavy metal ions Mn 5162.4 mg/g, heavy metal ions Fe 5849.4 mg/g, metal ions Zn 4894.22 mg/g and heavy metal ions Pb 468.2 mg/g. It can be seen from the order of adsorption capacity that Pb has the smallest capacity; this is proportional to the small % adsorption value so that it affects the weakest bond strength with CMC nanoadsorbents when compared to other heavy metal ions, such as Mn, Zn and Fe. Theoretically, the bond interaction between Pb ions and atoms of lone pair donor atoms, namely N atoms and O atoms, has the smallest ionic character or the largest covalent character, because it has the largest atomic radius compared to other heavy metal ions (Shen et al., 2009; Gutierrez & Hilt, 2017). On the basis of the table, the order of adsorption reactions for Pb, Mn, Zn, and Fe ions

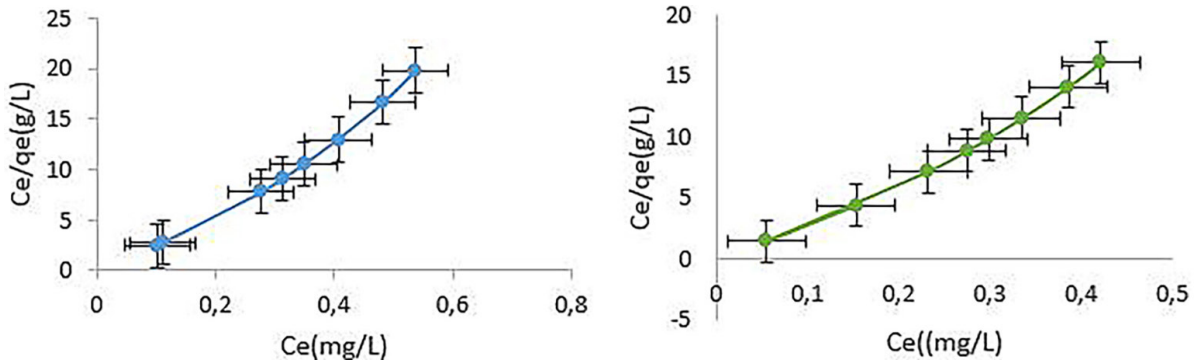

Figure 5. Relationship between Ce and Ceqe Langmuir adsorption model for heavy metals (a) Fe and (b) Mn

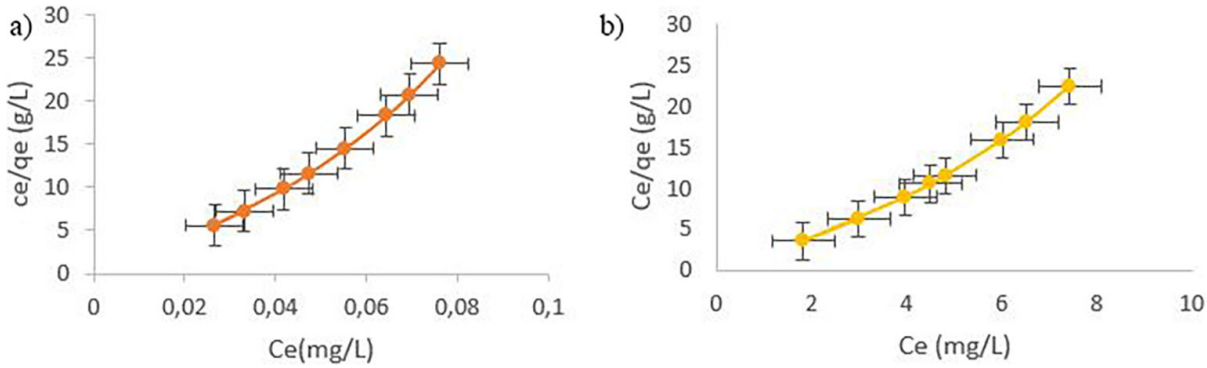

Figure 6. Relationship between Ce and Ceqe Langmuir adsorption model for heavy metals (a) Pb and (b) Zn

varies with pseudo-first order and pseudo-second order; this is due to the four heavy metal ions, the intensity of the four heavy metals being strong enough to interact with the CMC nanoadsorbent sample, in this case sample 4 of the four heavy metals, Pb has the lowest relative mobility compared to the other three heavy metal ions, Mn, Zn and Fe. Likewise, other heavy metal ions which have higher relative mobility tend to interact with higher binding affinity sites (O and N active groups) than interacting with lower binding affinity sites (Dave & Chopda, 2014; Wojciechowska, 2020). On the basis of the research, the lower the mobility of the heavy metal ion Pb, the longer the settling time at the two bonding sites when compared to other heavy metal ions Mn, Zn and Fe. In addition, the research reports successively from the lowest to the highest is Pb>Mn>Zn>Fe.

XRD

In the discussion of XRD nanoadsorbent CMC shown combined for 7 seven samples namely sample 1, sample 2, sample 3, sample 4, sample 5, sample 6 and sample 7. The results of the analysis with combined XRD are shown in Figure where almost the seven samples have a phase pattern the same peak/similar in that the structure is crystalline. The compounds formed are Fe_3O_4 and Fe_3C with different percentages for each sample.

The Debye-Scherrer scattering equation enables to estimate the mean crystal size of CMC nanoadsorbents, both S1, S2, S3, S4, S5, S6 and S7. The results of the crystal size analysis are shown in Table 2. It can be seen in Table 2 that all samples have a size towards the nanometer order and S4 has a smaller crystal size which is about 24.5 nm compared to other samples. It can be concluded that the crystal size affects the % adsorption value of heavy metal ions, where a small size will increase the % adsorption and the order from the largest to the smallest is S1>S2>S5>S7>S6>S3>S4. On the basis of these results, it seems that the Fe_3O_4 phase is the dominant phase in this sample S1, with the identification at a diffraction angle of 2θ 18,14°; 30,02°; 37,02°; 53,34° and 56,84°. identification for the Fe_3C phase at a diffraction angle of 26.56°, while the rest is the common phase, namely at a diffraction angle of 35,34° and 42,98°. Slightly different from sample S1, sample S2 can be seen in Figure where the image shows that the crystal system is

Table 2. Result data analysis of sample crystal size using Debye Scherrer

Sample	*K*	*λ*(A)	Peak position (2*θ* °)	FWHM (°)	*D* (nm)	*hkl*	*d*(A)
Sample 1	0.94	1.541874	35.34	0.2684	32.47175399	311	2.69157
Sample 2	0.94	1.541874	35.32	0.27044	32.2250198	311	4.66714
Sample 3	0.94	1.541874	35.58	0.35594	26.27396703	311	2.94647
Sample 4	0.94	1.541874	35.36	0.27096	24.50204165	311	2.08515
Sample 5	0.94	1.541874	35.38	0.33175	32.16675342	311	1.69152
Sample 6	0.94	1.541874	35.34	0.27096	31.82435833	311	1.60597
Sample 7	0.94	1.541874	35.52	0.27395	31.82987006	311	1.44555

cubic (a = 8.3837) for the Fe_3O_4 phase as much as 85.4% and orthorhombic (a = 4.5110, b = 5.0470, c = 6.7380) for Fe_3C as much as 14.6%. The percentage of magnetic phase is higher than that of the S1 sample. Identification at diffraction angle 18,10°; 30,02°; 53,34°; 56,88° and 62,46°. identification for the Fe_3C phase at a diffraction angle of 26,56°. Then, for the S3 sample the diffraction pattern can be seen in the figure, it can be seen that the crystal system is cubic (a = 8.3814) for the Fe_3O_4 phase as much as 81.7% and orthorhombic (a = 4.5110, b = 5.0470, c = 6, 7380) for Fe_3C as much as 18.3%. On the basis of these results, it seems that the Fe_3O_4 phase is also the more dominant phase in the S3 sample compared to the S1 sample, but not more than the S2 sample with identification at a diffraction angle of 2θ 18,24°; 30,20°; 37,28°; 53,58°; 57,14° and 62,70°. Identification for the Fe_3C phase is at a diffraction angle of 26.70°, while the rest is the common phase, namely at a diffraction angle of 35,58° and 43,28°. The image shows the crystal system is cubic (a = 8.3985) for the Fe_3O_4 phase as much as 69.2% and orthorhombic (a = 4.5110, b = 5,0470, c = 6.7380) for Fe_3C as much as 30.8%. It is the same with the previous S1, S2 and S3 samples where the pure magnetic phase is more abundant than the mixed carbon phase. However, the S4 sample was special, because at the time of measurement with AAS it also had a better performance than other samples in remediating polluted water with the highest adsorption % indication. In the discussion of the diffraction pattern in sample S4 also the percentage of Fe_3C is greater than the other samples, namely the diffraction angle of 2θ is the Fe_3O_4 phase of 30,02°; 36,98°; 53,22° and 62,46°. The Fe_3C phase was identified at a diffraction angle of 26,54°, while the rest is the common phase at a diffraction angle of 35,36°; 43,00°; and 56,92°. Sample S5 shows that the crystal system is cubic (a = 8.3862) for the Fe_3O_4 phase as much as 70.5% and orthorhombic

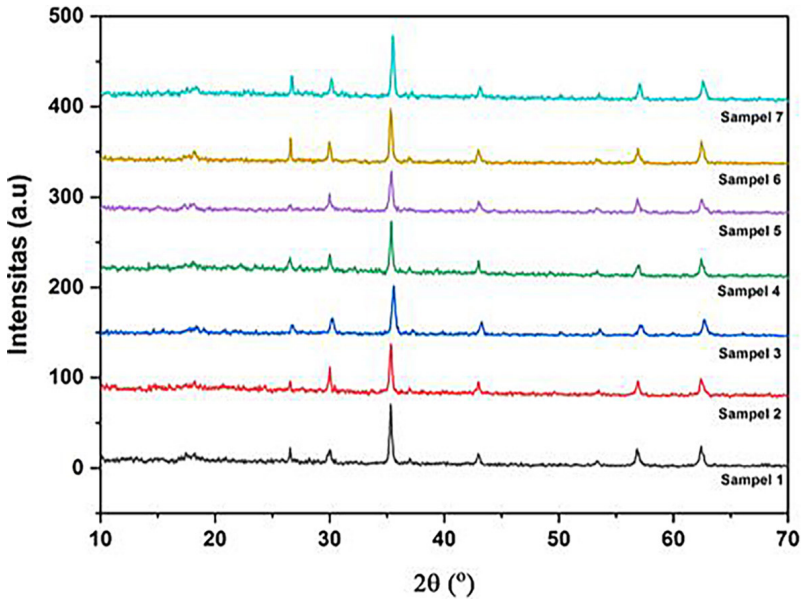

Figure 7. Diffraction pattern of CMC nanoadsorbent

(*a* = 4.5110, *b* = 5.0470, *c* = 6.7380) for Fe_3C as much as 29,5%. The percentage of the magnetic phase is still lower than samples S1, S2 and S3 but larger than samples S4. The Fe_3O_4 phase can be identified at diffraction angles of 18.16°, 29.96°, 53.38°, 53.58°, and 62.48° Identification for the Fe_3C phase is at a diffraction angle of 26.56°, while the rest is the common phase, namely at a diffraction angle of 35.38°, 43.00° and 56.86°. Sample S6 has a Fe_3O_4 phase percentage as much as 79.8% and for Fe3C as much as 20.2% with the crystal systems are cubic (*a* = 8.3740) and orthorhombic (a = 4.5110, *b* = 5.0470, *c* = 6.738. The Fe_3O_4 phase can be identified at diffraction angles of 18,14°; 29,98°; 36,94; 53,42°; 56,90° and 62,48°. Identification for the Fe_3C phase at a diffraction angle of 26,58°, while the rest is the shared phase at an angle diffraction 35,34° and 42,96°.

The last is sample S7, where this sample is relatively similar to samples S1 and S6, having a percentage of Fe_3O_4 phase as much as 78.2% and for Fe_3C as much as 21.8% with the crystal system being cubic (a = 8.3740) and orthorhombic (*a* = 4.5110, *b* = 5.0470, *c* = 6.7380). The Fe_3O_4 phase can be identified at diffraction angles of 18,14°; 29,98°; 36,94; 53,42°; 56,90° and 62,48°. Identification for the Fe_3C phase at a diffraction angle of 26,72°, while the rest is the common phase, namely at a diffraction angle of 35,52° and 43,12°. From the seven sample analyses, it can be said that sample S4 has a smaller Fe_3O_4 phase than samples S1,S2,S3, S5, S6 and S7 and the Fe_3C phase is larger than the other samples It can be judged that sample S4 is the optimal sample with a ratio of 1:2:2. The phases formed in the XRD results strengthen the hypothesis that the CMC nanoadsorbent incorporation method is suitable for synthesizing these three materials (Amin et al., 2014; Gutierrezet al., 2017). For this reason, the S4 sample was carried out advanced characterization, namely SEM/EDX, FTIR, PSA, TGA, and BET.

SEM/EDX

The surface morphology and microstructure of the S4 sample synthesized by combining three materials, namely chitosan, magnetic and banana peel activated carbon (1:2:2) were observed using a scanning microscope (SEM) as shown in Figure 8. On the basis if on the SEM results, it can be seen that the microstructure of the material resembles islands and small grains around them; it is predicted using software that the islands are dominated by activated carbon of banana peels combined with Fe, namely Fe_3C and the surrounding small grains are Fe_3O_4. There is a lot of agglomeration on the surface of the sample (Lin et al., 2020; Chibowski, 2018). From the previous analysis, banana peel activated carbon is a porous material, so it can be seen that the pores are filled with magnetic Fe_3O_4. Sample S4 was characterized by SEM having an average particle size in the range of 2–10 µm. Magnification was performed on the SEM 2000× tool. To see the elemental content in the S4 sample, further testing was carried out on SEM with EDX,

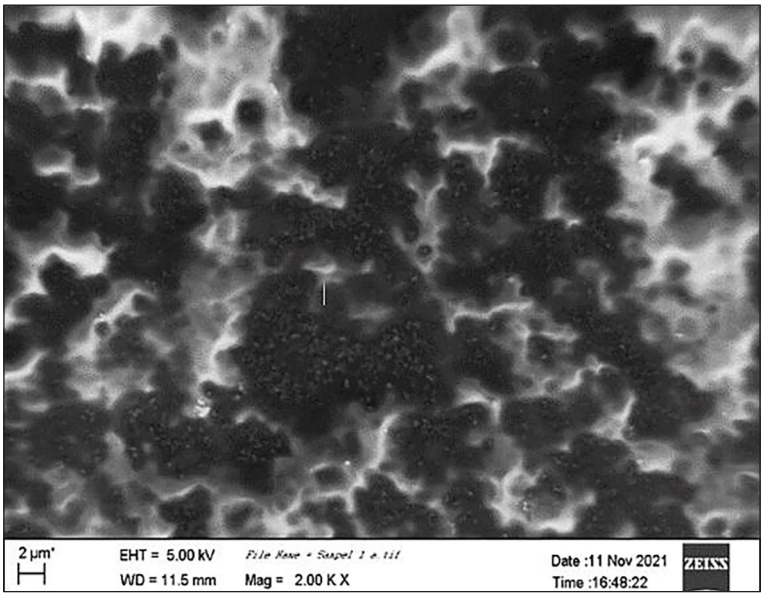

Figure 8. Surface morphological data of CMC S4 nanoadsorbent with a magnification of 2000×

the results are as shown in Figure 9. The EDX results to determine the elemental content of the S4 nanoadsorbent CMC sample, Fe, C and O elements were obtained.

The Fe and O elements came from Fe_3O_4 magnetic material synthesized by the coprecipitation method, while the C element came from banana peel activated carbon synthesized by the combination method (Lesaoana et al., 2019; Blue et al., 2021). The percentage of elements from the S4 nanoadsorbent CMC sample as seen in Figure 9 is Fe elements as much as 57.25%, C elements as much as 26.50% and O elements as much as 16.25%. This shows that the S4 sample has elemental purity without any other elemental impurities.

FTIR

The results of the analysis of the S4 nanoadsorbent CMC sample using FTIR are shown in Figure 10. The wavelength in Figure 10 is the transmittance of 3880.45; 3440.77; 2968.33; 2813.47; 2417.88; 1746.55; 1441.36; 1050.11; 908.34; 796.81; 598.16 cm^{-1}. The spectrum in Figure 3.10 confirms that the hydrogen stretching vibrational environment exists at the wavelengths of 3880.45 and 3440.77 cm^{-1}. Hydrogen bonding causes the peak to widen and a shift occurs towards a shorter wave number, namely 2968.33; 2813.47; 2417.88, so that it experienced absorbance (Lin & Jiang, 2019; Manyangadze et al., 2020). Changes in the structure of the C-H, NH, O-H bonds will cause the peak to shift towards the maximum. The hydrogen on the carbonyl group of the aldehyde gives peaks at 1746.55 and 1441.36 cm^{-1}. This shows that the glutaraldehyde material has the ability to bind strongly to the three materials, as it is known that the material has crosslinking properties. Another active group is at 1050.11; 908.34; 796.81; 598.16 cm^{-1} which is C-C and C-O in the form of bending vibrations (buckling). From the description, it can be seen that the combined synthesis of the three CMC materials produces hydroxyl, carboxyl and aldehyde active functional groups.

PSA

The results of characterization and calculations using scattering technique software using PSA obtained the average particle size distribution of CMC nanoadsorbents were (10%) 40 nm, (50%) 300 nm, and (90%) 400 nm. Then the average particle size of the CMC nanoadsorbent is around 150.4 nm which is included in the fine particle category. For this reason, this sample can be said to be nanoparticle size (Danish et al., 2018; Dave & Chopda, 2014). The particle size distribution can be seen in Figure 11.

BET-BJH

The results of the BET (Brunaeur Emmet Teller) and BJH (Barret Joyner Halende) tests showed that the specific surface area was 450.8 m^2/g. BJH D-H Adsorption cumulative volume of pores between 1.7000 nm and 300,0000 nm diameter is 0.202 m^3/g. BJH D-H Desorption cumulative surface area of pores between 1,7000 nm and 300,0000 nm diameter is 0.411 m^3/g, while the pore diameter is 2.13 nm. The particle size of the sample was 13.312 nm. On the surface of the S4 nanoadsorbent

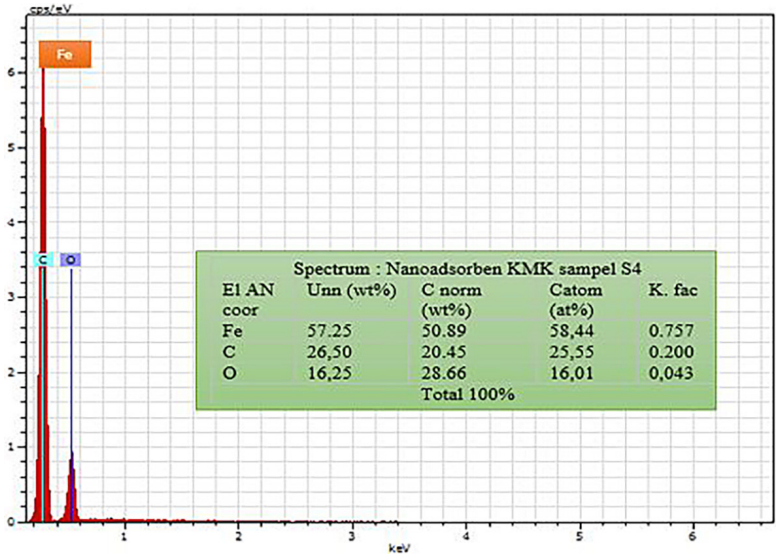

Figure 9. EDX results of S4 CMC nanoadsorbent samples

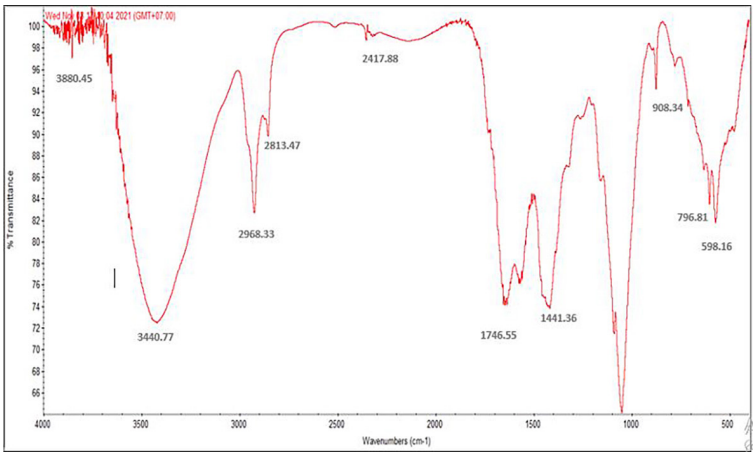

Figure 10. FTIR Spectrum of S4 nanoadsorbent CMC samples

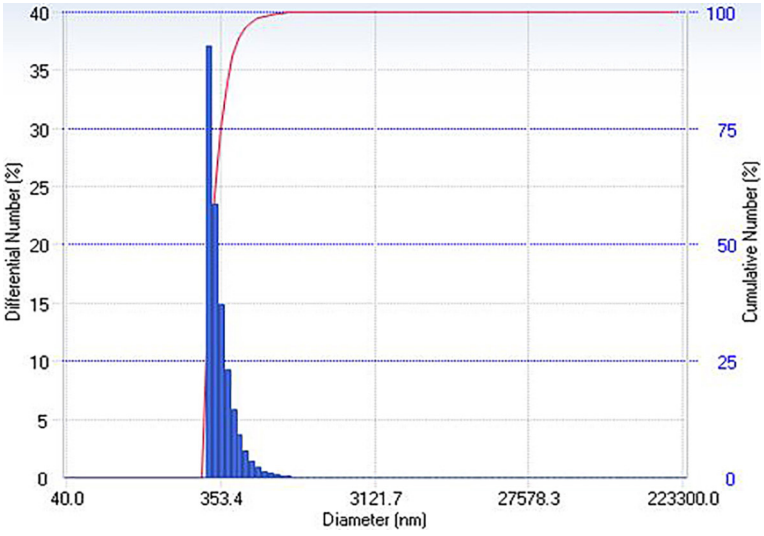

Figure 11. Particle size distribution graph of CMC nanoadsorbent

CMC sample, there was a very drastic increase in nitrogen gas adsorption and was known as a hysterical loop which stated the characteristics of the mesoporous diameter. On the basis on the measurement results, this sample is classified as mesoporous (2–50 nm). The area of the S4 nanoadsorbent CMC sample is larger than that of the banana peel activated carbon sample (Chibowski, 2018; Lin & Jiang, 2019; Shukla et al., 2020). In theory, the increase in surface area will affect the amount of adsorbate adsorbed, in this case the four heavy metal ions, i.e. Fe, Pb, Mn and Zn. Nanoadsorbents have strength because of their high adsorption activity on heavy metal ions, judging from the ability of oxygen, hydrogen and carbon sites as free electron donors resulting in strong heavy metal ion bonds on the surface of the S4 nanoadsorbent CMC sample. In the characterization of BET/BJH obtained isothermically using the Freundlich method Qm C: 0.0331 ± 0.0013 cm³/g STP m: 3.6407 ± 0.2663 and Temkin q·alpha/Qm: 22.803921 ± 0.655982 kJ/ mol·(cm³/g STP) A: 0.7216 ± 0.0960 mmHg.

TGA

The following is a TGA graph that states the relationship between sample temperature and % TG (weight) of the S4 nanoadsorbent CMC sample. From the TGA graph in Figure 12 it can be seen that the S4 nanoadsorbent CMC sample has a fairly high resistance to the decomposition process, because the weight loss is still around 30% of 100% TG sample. The temperature used during the test is 25–500 °C. The heating rate used is 10° min using oxygen gas (Matome et al., 2020; Drbohlavova et al., 2010). The resistance of this S4 sample to the decomposition process indicates that there is an interaction through intermolecular hydrogen bonds between the active groups of the S4 nanoadsorbent CMC sample mixture consisting of chitosan, magnets and banana peels activated carbon (Koesnarpadi et al., 2015).

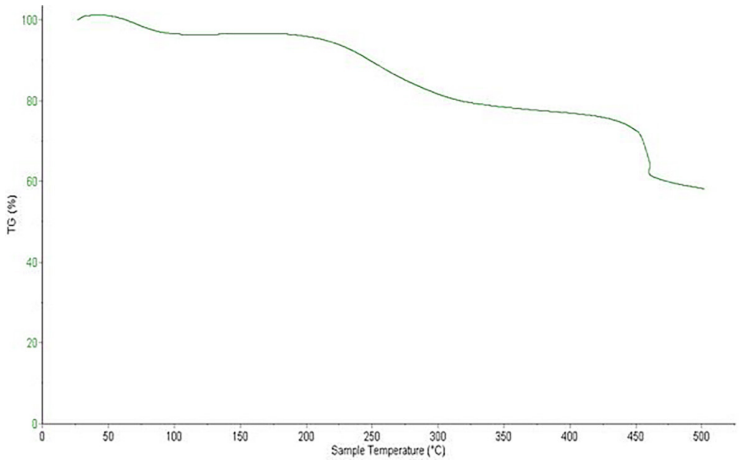

Figure 12. % TG vs sample temperature of S4 nanoadsorbent CMC samples

CONCLUSIONS

In accordance with the research objectives, from the results of the study it was concluded that CMC nanoadsorbent can optimally remediate water contaminated with heavy metals Fe, Mn, Zn and Pb when compared to magnetic adsorbents and banana peel activated carbon alone. The increase occurred when both were combined and chitosan was added. The optimum adsorption time for each heavy metal ion, i.e. Fe, Mn, Zn and Pb, is 210 min. The most effective sample is sample S4 for each adsorbed heavy metal ion with the highest adsorption of 95.44% for Fe. The Langmuir model for Fe, Mn, Zn and Pb ions shows a curved graph, this curvature as evidence of surface heterogeneity of the bonding sites of CMC nanoadsorbents. The maximum adsorption capacity using the Langmuir method is for the highest heavy metal ion and Fe 5849.4 mg/g. The adsorption kinetics showed that the reaction order for Pb, Mn, Zn, and Fe ions varied with pseudo first order and pseudo second order. On the basis of the results of the characterization of nanoadsorbent CMC sample S4 which has a crystal size specification of about 24 nm, particle size of 150.4 nm, pore size of 2 nm, specific surface area of 450.8 m²/g. %, element C as much as 26.50% and element O as much as 16.25 %, the FTIR spectrum confirmed that the sample produced active functional groups of hydroxyl, carboxyl and aldehyde and had a fairly high resistance to the decomposition process.

Acknowledgments

Thank to the Directorate General of Resources for Science, Technology and Higher Education for trusting. The author to get a scholarship for the BP-PDN doctoral program. Thanks to the Deputy for Strengthening Research and Development under contract number 059/E5/PG.02.00/PT/2022 and the Muslim Nusantara Alwasliyah University for providing PDD grants for this research to be completed optimally.

REFERENCES

1. Abbasi, M. 2017. Synthesis and characterization of magnetic nanocomposite of chitosan/SiO2/carbon nanotubes and its application for dyes removal Mahmoud. Journal of Cleaner Production. https://doi.org/10.1016/j.jclepro.2017.01.046
2. Adusei, J.K., Agorku, E.S., Voegborlo, R.B., Ampong, F.K., Danu, B.Y., Amarh, F.A. 2022. Removal of Methyl red in aqueous systems using synthesized NaAlg-g-CHIT/nZVI adsorbent. Scientific African, 17, e01273. https://doi.org/10.1016/j.sciaf.2022.e01273
3. Wojciechowska, A., Lendzion, Z.B. 2020. Synthesis and Characterization of Magnetic Nanomaterials with Adsorptive Properties of. Molecules, (III).
4. Alinezhad, H., Zabihi, M., Kahfroushan, D. 2020. Design and fabrication the novel polymeric magnetic boehmite nanocomposite (boehmite@ Fe3O4@ PLA@SiO2) for the remarkable competitive adsorption of methylene blue and mercury ions. Journal of Physics and Chemistry of Solids, 144(December 2019), 109515. https://doi.org/10.1016/j.jpcs.2020.109515
5. Amin, M.T., Alazba, A.A., Manzoor, U. 2014. A Review of Removal of Pollutants from Water / Wastewater Using Different Types of Nanomaterials. Advanced in Materials Science and Engineering, 2014.
6. Annadurai, G., Juang, R.S., Lee, D.J. 2018. Adsorption of Heavy Metals From Water Using Banana

and Orange Peels (PDF Download Available). Water Science and Technology, (July), 185–190.

7. Blue, C.F.O.P., Long, X., Chen, H., Huang, T., Zhang, Y., Lu, Y., Chen, R. (2021). Removal of Cd (II) from Micro-Polluted Water by Magnetic. Molecules, (II).
8. Chen, A., Shang, C., Shao, J., Lin, Y., Luo, S., Zhang, J., Huang, H. 2017. Carbon disulfide-modified magnetic ion-imprinted chitosan-Fe (III): A novel adsorbent for simultaneous removal of tetracycline and cadmium. Carbohydrate Polymers, 155, 19–27. https://doi.org/10.1016/j.carbpol.2016.08.038
9. Chibowski, E. 2018. Magnetic Water treatment-a review of the latest approaches. Chemosphere. https://doi.org/10.1016/j.chemosphere.2018.03.160
10. Danish, M., Ahmad, T., Majeed, S., Ahmad, M., Ziyang, L., Pin, Z., Shakeel Iqubal, S.M. 2018. Use of banana trunk waste as activated carbon in scavenging methylene blue dye: Kinetic, thermodynamic, and isotherm studies. Bioresource Technology Reports, 3, 127–137. https://doi.org/10.1016/j.biteb.2018.07.007
11. Dave, P.N., Chopda, L.V. 2014. Application of Iron Oxide Nanomaterials for the Removal of Heavy Metals. Journal of Nanotechnology, 2014.
12. Drbohlavova, J., Hrdy, R., Adam, V., Kizek, R., Schneeweiss, O., Hubalek, J. 2010. Preparation and properties of various magnetic nanoparticles. Sensors, 9(4), 2352–2362. https://doi.org/10.3390/s90402352
13. Feng, X., Sun, S., Cheng, G., Shi, L., Yang, X., Zhang, Y. 2021. Removal of Uranyl Ion from Wastewater by Magnetic Adsorption Material of Polyaniline Combined with CuFe 2 O 4. Adsorption Science & Technology, 2021.
14. Gameli, B.H.R., Duwiejuah, A.B., Bawa, A.A. 2022. Adsorption of toxic metals from greywater using low-cost spent green tea as a novel adsorbent. Scientific African, 17, e01296. https://doi.org/10.1016/j.sciaf.2022.e01296
15. Gutierrez, A.M., Dziubla, T.D., Hilt, J.Z. 2017. Recent advances on iron oxide magnetic nanoparticles as sorbents of organic pollutants in water and wastewater treatment, 32, 111–117. https://doi.org/10.1515/reveh-2016-0063
16. Gutierrez, A.M., Hilt, J.Z. 2017. Recent Advances on Iron Oxide Magnetic Nanoparticles as Sorbents of Organic Pollutants in Water and Wastewater Treatment Recent Advances on Iron Oxide Magnetic Nanoparticles as Sorbents of Organic. Reviews on Envirinmental Health.
17. Hu, B., Ai, Y., Jin, J., Hayat, T., Alsaedi, A., Zhuang, L., Wang, X. 2020. Efficient elimination of organic and inorganic pollutants by biochar and biochar-based materials. Biochar, 2(1), 47–64. https://doi.org/10.1007/s42773-020-00044-4
18. Khairiah, K., Frida, E., Sebayang, K., Sinuhaji, P., Humaidi, S. 2021. Data on Characterization, Model, and Adsorption Rate of Banana Peel Activated Carbon (Musa Acuminata) for Adsorbents of Various Heavy Metals (Mn, Pb, Zn, Fe). Data in Brief, 39, 107611. https://doi.org/10.1016/j.dib.2021.107611
19. Khairiah, K., Frida, E., Sebayang, K., Sinuhaji, P., Humaidi, S., Fudholi, A. 2021. The Development of a Novel FM Nanoadsorbent for Heavy Metal Remediation in Polluted Water. South African Journal of Chemical Engineering, 39(July 2021), 32–41. https://doi.org/10.1016/j.sajce.2021.11.006
20. Koesnarpadi, S., Juari, S., Siswanta, D., Rusdiarso, B. 2015. Synthesis and characterizatation of magnetite nanoparticle coated humic acid (Fe3O4 / HA). Procedia Environmental Sciences, 30, 103–108. https://doi.org/10.1016/j.proenv.2015.10.018
21. Lesaoana, M., Mlaba, R.P.V, Mtunzi, F.M., Klink, M.J., Ejidike, P., Pakade, V.E. 2019. Influence of inorganic acid modification on Cr (VI) adsorption performance and the physicochemical properties of activated carbon. South African Journal of Chemical Engineering, 28(January), 8–18. https://doi.org/10.1016/j.sajce.2019.01.001
22. Lin, L., Jiang, W. (n.d.). A critical review of the application of electromagnetic fi elds for scaling control in water systems : mechanisms, characterization, and operation. Npj Clean Water. https://doi.org/10.1038/s41545-020-0071-9
23. Lin, S., Jin, J., Sun, S., Yu, J. 2020. Removal of arsenic contaminants using a novel porous nanoadsorbent with superior magnetic recovery. Chemical Engineering Science: X, 8, 100069. https://doi.org/10.1016/j.cesx.2020.100069
24. Mahmoudi, F., Amini, M.M., Sillanpää, M. 2020. Synthesis of MIL-100 (Fe)/ SBA-15 composite as a novel and ultrafast adsorbent for removal of methylene blue dye from aqueous solution. Inorganic Chemistry Communications, 100, 108032. https://doi.org/10.1016/j.inoche.2020.108032
25. Manyangadze, M., Chikuruwo, N.H.M., Narsaiah, T.B., Chakra, C.S., Radhakumari, M., Danha, G. 2020. Enhancing adsorption capacity of nano-adsorbents via surface modi fi cation : A review. South African Journal of Chemical Engineering, 31(September 2019), 25–32. https://doi.org/10.1016/j.sajce.2019.11.003
26. Matome, S.M., Makhado, E., Katata-Seru, L.M., Maponya, T.C., Modibane, K.D., Hato, M.J., Bahadur, I. 2020. Green synthesis of polypyrrole / nanoscale zero valent iron nanocomposite and use as an adsorbent for hexavalent chromium from aqueous solution. South African Journal of Chemical Engineering, 34(November 2019), 1–10. https://doi.org/10.1016/j.sajce.2020.05.004
27. Munagapati, V.S., Yarramuthi, V., Kim, Y., Lee, K.M.,

Kim, D.S. 2018. Removal of anionic dyes (Reactive Black 5 and Congo Red) from aqueous solutions using Banana Peel Powder as an adsorbent. Ecotoxicology and Environmental Safety, 148(August 2017), 601–607. https://doi.org/10.1016/j.ecoenv.2017.10.075

28. Negroiu, M., Țurcanu, A.A., Matei, E., Râpă, M., Covaliu, C.I., Predescu, A.M., Predescu, C. 2021. Novel Adsorbent Based on Banana Peel Waste for Removal of Heavy Metal Ions from Synthetic Solutions. Materials, 14(14), 3946. https://doi.org/10.3390/ma14143946
29. Nithya, R., Sudha, P.N. 2016. Removal of heavy metals from tannery effluent using chitosan-g-poly (butyl acrylate)/ bentonite nanocomposite as an adsorbent. Textiles and Clothing Sustainability, 1–8. https://doi.org/10.1186/s40689-016-0018-1
30. Olaoye, R.A., Afolayan, O.D., Adeyemi, K.A., Ajisope, L.O., Adekunle, O.S. 2020. Adsorption of selected metals from cassava processing wastewater using cow-bone ash. Scientific African, 10, e00653. https://doi.org/10.1016/j.sciaf.2020.e00653
31. Petcharoen, K., Sirivat, A. 2012. Synthesis and characterization of magnetite nanoparticles via the chemical co-precipitation method. Materials Science and Engineering B: Solid-State Materials for Advanced Technology, 177(5), 421–427. https://doi.org/10.1016/j.mseb.2012.01.003
32. Safari, E., Rahemi, N., Kahforoushan, D., Allahyari, S. 2019. Copper adsorptive removal from aqueous solution by orange peel residue carbon nanoparticles synthesized by combustion method using response surface methodology. Journal of Environmental Chemical Engineering, 7(1), 102847. https://doi.org/10.1016/j.jece.2018.102847
33. Saleh Jafer, A., Hassan, A.A. 2019. Removal of oil content in oilfield produced water using chemically modified kiwi peels as efficient low-cost adsorbent. Journal of Physics: Conference Series, 1294(7). https://doi.org/10.1088/1742-6596/1294/7/072013
34. Shen, Y.F., Tang, J., Nie, Z.H., Wang, Y.D., Ren, Y., Zuo, L. 2009. Preparation and application of magnetic Fe3O4 nanoparticles for wastewater purification, 68, 312–319. https://doi.org/10.1016/j.seppur.2009.05.020
35. Shukla, S.K., Al Mushaiqri, N.R.S., Al Subhi, H.M., Yoo, K., Al Sadeq, H. 2020. Low-cost activated carbon production from organic waste and its utilization for wastewater treatment. Applied Water Science, 10(2), 1–9. https://doi.org/10.1007/s13201-020-1145-z
36. Singh, S., Parveen, N., Gupta, H. 2018. Adsorptive decontamination of rhodamine-B from water using banana peel powder: A biosorbent. Environmental Technology and Innovation, 12, 189–195. https://doi.org/10.1016/j.eti.2018.09.001
37. Siregar, J., Septiani, N.L.W., Abrori, S.A., Sebayang, K., Irzaman, Fahmi, M.Z., Yuliarto, B. 2021. Review—A Pollutant Gas Sensor Based On Fe3O4 Nanostructures: A Review. Journal of the Electrochemical Society, 168(2), 027510. https://doi.org/10.1149/1945-7111/abd928
38. Tejada-Tovar, C., Gonzalez-Delgado, A., Villabona-Ortiz, A. 2018. Comparison of banana peel biosorbents for the removal of Cr (VI) from water. Contemporary Engineering Sciences, 11(21), 1033–1041. https://doi.org/10.12988/ces.2018.8390
39. Yu, S., Pang, H., Huang, S., Tang, H., Wang, S., Qiu, M., Wang, X. 2021. Recent advances in metal-organic framework membranes for water treatment: A review. Science of the Total Environment, 800, 149662. https://doi.org/10.1016/j.scitotenv.2021.149662
40. Yuvaraja, G., Venkata, M. 2016. Removal of Pb (II) ions by using magnetic chitosan-4- ((pyridin-2-ylimino) methyl) benzaldehyde Schiff's base. International Journal of Biological Macromolecules, 93, 408–417. https://doi.org/10.1016/j.ijbiomac.2016.08.084